

**\*\*FULL TITLE\*\***

*ASP Conference Series, Vol. \*\*VOLUME\*\*, \*\*YEAR OF PUBLICATION\*\**

**\*\*NAMES OF EDITORS\*\***

## **Cosmic Infrared Background: Resolved, Unresolved and *Spitzer* Contributions.**

Hervé Dole, Guilaine Lagache, Jean-Loup Puget

*Institut d'Astrophysique Spatiale, bâtiment 121, Université Paris Sud  
XI, F-91405 Orsay Cedex, France*

**Abstract.** The Cosmic Infrared Background (CIB) peaks in the Far-Infrared (FIR), and its Spectral Energy Distribution (SED) is now well constrained. Thanks to recent facilities and *Spitzer*, the populations contributing to the CIB are being characterized: the dominant galaxy contributions to the FIR CIB are Luminous IR galaxies (LIRGs) at  $0.5 \leq z \leq 1.5$  and, to the submm CIB, Ultra-LIRGs at  $z \geq 2$ . These populations of galaxies experience very high rates of evolution with redshift. Because of confusion, the CIB is (and will remain in some domains) partially resolved and its contributing galaxies SEDs are not well constrained. We discuss all these aspects and show how confusion limits *Spitzer* observations, and how to overcome it in order to study the unresolved part of the CIB.

### **1. Introduction**

A Cosmic Background that would trace the peak of the star-formation and metal production in galaxy assembly has long been predicted. Its discovery in 1996 by Puget et al. (see the review by Hauser & Dwek 2001), together with recent cosmological surveys in the infrared (IR) and submillimeter, has revolutionized our view on star formation at high redshift. It has become clear that a population of galaxies radiating most of their power in the far-IR (the so-called “IR galaxies”) contributes an important part of the whole galaxy build-up in the Universe. Since 1996, detailed (and often painful) investigations of the high-redshift IR galaxies have resulted in spectacular results that are reviewed in Lagache et al. (2005). In this paper we detail briefly the sources of the Cosmic IR Background (CIB, Sect. 2) and their average evolution properties (Sect. 3). We discuss the extragalactic confusion noise, one of the most limiting factor of Far-IR cosmological surveys (Sect. 4) and give first hints on how we can overcome it with *Spitzer* and other facilities (Sect. 5).

### **2. Sources of the Cosmic IR Background: Redshift Distributions**

The full Cosmic Extragalactic Background Spectral Energy Distribution (SED) is shown in figure 1. For clarity, we only plotted the most recent and strongly constraining measurements. The figure clearly shows that the optical and the IR cosmic backgrounds are well separated. The first surprising result is that the power of the IR part (the CIB, Cosmic IR Background) is comparable to the power of the optical one, although we know that locally the IR output of galaxies

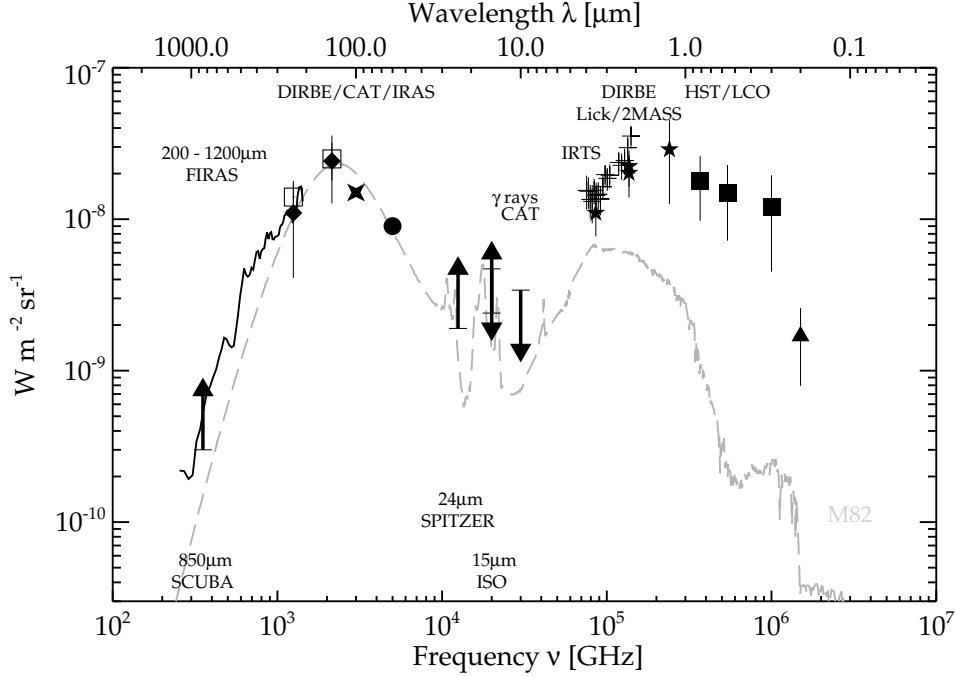


Figure 1. The extragalactic background over 3 decades of frequencies from the ultraviolet to millimeter wavelengths. Only strongly constraining measurements have been reported. We show for comparison in gray an SED of M82 (Chanial, 2003), a starburst galaxy at  $L=3 \cdot 10^{10} L_{\odot}$ , normalized to the peak of the CIB at  $140 \mu m$ . CIB measurements are, by decreasing frequency: Armand et al. (1994) at  $2000 \text{ \AA}$ ; Bernstein et al. (2002) at 300, 555 and 814 nm using the *HST* and Las Campanas Observatory; Mastumoto et al. (2004) between 2.2 and  $4 \mu m$  using the *IRTS*; Gorjian et al. (2000) at 2.2 and  $3.3 \mu m$  using *DIRBE* and *Lick*; Wright (2001) at 1.25 and  $2.2 \mu m$  using *DIRBE* and *2MASS*; Renault et al. (2001) upper limits at 10 and  $15 \mu m$  using the *CAT* in the  $\gamma$ -rays; Elbaz et al. (1999) lower limit at  $15 \mu m$  using galaxy counts with *ISOCAM*; Papovich et al. (2004) lower limit at  $24 \mu m$  using galaxy counts with *Spitzer/MIPS*; An estimate of the CIB at  $60 \mu m$  from Miville-Deschênes et al. (2002) using *IRAS*; Renault et al. (2001) at  $100 \mu m$  using *CAT* and *DIRBE*; Lagache et al. (2000) at 140 and  $240 \mu m$  using *DIRBE* and *WHAM*; Hauser et al. (1998) at 140 and  $240 \mu m$  using *DIRBE*; Smail et al. (2002) lower limit at  $850 \mu m$  using galaxy counts with *SCUBA*; Lagache et al. (2000) spectrum between  $200 \mu m$  and  $1.2 \text{ mm}$  using *FIRAS*.

is only one third of the optical (Soifer & Neugebauer 1991). This implies a much stronger evolution of the IR luminosity of IR galaxies than of the optical ones. A second important property to notice is the long wavelength ( $\lambda \geq 200 \mu m$ ) behavior: the CIB slope ( $B_{\nu} \propto \nu^{1.4}$ , Gispert et al. 2000), is much shallower than the long wavelength spectrum of galaxies (fig. 1). This implies that the millimeter CIB is not due to the millimeter emission of the galaxies making the bulk of the emission at the peak of the CIB (at  $\sim 170 \mu m$ ). The implications in terms of energy output have been drawn by e.g. Gispert et al. (2000). The IR production rate per comoving unit volume 1) evolves faster between redshift

zero and 1 than the optical one and 2) has to stay constant at higher redshifts up to redshift 3 at least.

In figure 1, showing the CIB and a galaxy SED, we see that contributions from galaxies at various redshifts are needed to fill the CIB SED shape. The bulk of the CIB in energy, i.e. the peak at about  $150\ \mu\text{m}$ , is not yet resolved in individual sources, but one dominant contribution to the CIB peak can be inferred from the *ISOCAM* deep surveys. *ISOCAM* galaxies with a median redshift of  $\sim 0.7$  resolve about 80% of the CIB at  $15\ \mu\text{m}$ . Elbaz et al. (2002) separate the  $15\ \mu\text{m}$  galaxies into different classes (ULIRGs, LIRGs, Starbursts, normal galaxies and AGNs) and extrapolate the  $15\ \mu\text{m}$  fluxes to  $140\ \mu\text{m}$  using template SEDs. A total brightness of  $(16 \pm 5)\ \text{nW m}^{-2}\ \text{sr}^{-1}$  is found, that makes about two thirds of the CIB observed value at  $140\ \mu\text{m}$  by *COBE/DIRBE*. Hence, the galaxies detected by *ISOCAM* are responsible for a large fraction of energy of the CIB. About one half of the  $140\ \mu\text{m}$  CIB is due to LIRGs and about one third to ULIRGs. However, these *ISOCAM* galaxies make little contribution to the CIB in the millimeter and submillimeter. At those wavelengths, the CIB must be dominated by galaxies at rather high redshift for which the SED peak is shifted. This effect and the redshift contribution to the CIB are illustrated in figure 2. We clearly see that the submillimeter/millimeter CIB contains information on the total energy output by high-redshift galaxies ( $z > 2$ ). This is supported by the observed redshift distribution of the *SCUBA* sources at  $850\ \mu\text{m}$  that makes about 60% of the CIB and have a median redshift of 2.4 (Chapman et al. 2003).

Wavelength	20%	50%	80%
$15\ \mu\text{m}$	0.5	1.0	1.3
$24\ \mu\text{m}$	0.5	1.3	2.0
$70\ \mu\text{m}$	0.5	1.0	1.5
$100\ \mu\text{m}$	0.7	1.0	1.7
$160\ \mu\text{m}$	0.7	1.3	2.0
$350\ \mu\text{m}$	1.0	2.0	3.0
$850\ \mu\text{m}$	2.0	3.0	4.0
$1.4\ \text{mm}$	2.5	3.5	4.5
$2.1\ \text{mm}$	2.0	3.5	5.0

Table 1. Redshift at which the Cosmic IR Background is resolved at 20, 50 or 80%. Numbers have been derived using the model of Lagache et al. (2004).

Fifty percents of the CIB are made by galaxies at redshift below 1 at  $15$  and  $70\ \mu\text{m}$ , below 1.3 at  $24$  and  $160\ \mu\text{m}$  and below 2, 3 and 3.5 at  $350$ ,  $840$  and  $2000\ \mu\text{m}$  (see also Table 1). It is clear that, from the far-IR to the millimeter, the CIB at longer wavelength probes sources at higher redshifts.

So far, the most constraining surveys (in terms of resolving the CIB) are done at  $15$ ,  $24$  and  $850\ \mu\text{m}$  with *ISOCAM* (*ISO*), *MIPS* (*Spitzer*) and *SCUBA* (*JCMT*). The deep field observations resolve about 80, 70 and 60% of the CIB, respectively (Elbaz et al., 2002; Papovich et al., 2004; Smail et al., 2002). As shown above, these surveys probe the CIB in well-defined and distinct redshift ranges, with median redshift of 0.7 (Liang et al. 2004),  $\sim 1.1$  (L. Yan, priv. comm.), and 2.4 (Chapman et al. 2003) at  $15$ ,  $24$  and  $850\ \mu\text{m}$  respectively.

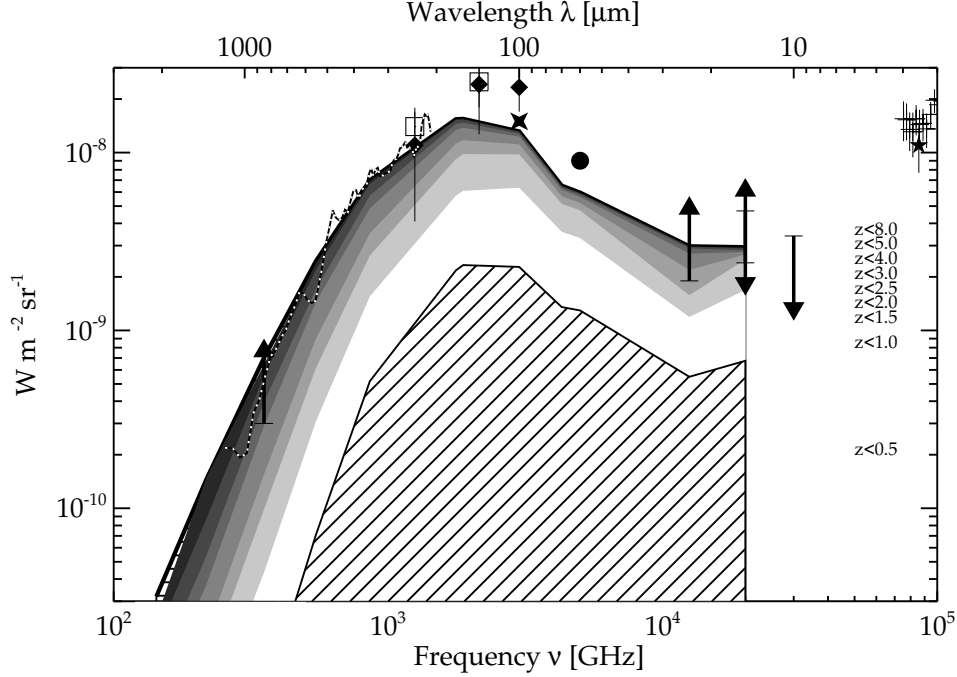


Figure 2. Cumulative contribution by redshift (from 0.5 to 8) of galaxies to the Cosmic IR Background, from the model of Lagache et al. (2004). Measurements of the CIB are reported with the same symbols as in figure 1, except for the *FIRAS* spectrum, represented in black and white dashes for visibility.  $z < 0.5$ : oblique shaded area;  $z < 1.0$ : white area;  $z < 1.5, 2.0, 2.5, 3.0, 4.0, 5.0$ : darker gray areas;  $z < 8$ : solid line and horizontal shaded region. Notice the non negligible contribution of  $5 < z < 8$  galaxies to the CIB, at wavelengths above  $600 \mu\text{m}$ .

Such well-defined redshift range selection can be understood by looking at the K-corrections (defined as  $K(L, z) = \frac{L_{\nu(1+z)}}{L_{\nu(z=0)}}$  where  $L_{\nu(z=0)}$  is the rest-frame luminosity). This correction is specific of the spectrum of the population considered at a given luminosity and redshift. Taking the standard SEDs of local normal starbursting galaxies (i.e. with PAHs features in the mid-IR), we observe in the K-correction at  $15 \mu\text{m}$  a hump at  $z \sim 1$  associated with the coincidence of the 6 to  $9 \mu\text{m}$  aromatic features and the *ISOCAM* filter, and at  $24 \mu\text{m}$  a hump at the same redshift for the  $24 \mu\text{m}$  *MIPS* filter associated with the 11- $14 \mu\text{m}$  set of aromatic features. Furthermore, a second hump is expected for the *MIPS*  $24 \mu\text{m}$  filter at  $z \sim 2$ , which corresponds to the redshifted 6 to  $9 \mu\text{m}$  features centered on this *MIPS* filter (Dole et al., 2003; Lagache et al., 2004). There is still a debate concerning the presence of this second hump in the  $24 \mu\text{m}$  sources redshift distribution observations (e.g. Pérez-González et al. 2005 vs L. Yan & P. Choi, *this volume*), even if growing evidences show the existence of PAHs at large redshift (e.g. Elbaz et al., 2005). At longer wavelengths, in the submillimeter and millimeter, the negative K-correction becomes very effective leading

to an almost constant observed flux for galaxies of the same total IR luminosity between redshifts 1 and 5.

### 3. Infrared Galaxy Cosmic Evolution

A remarkable property of the IR galaxies is their extremely high rates of evolution with redshift, exceeding those measured for galaxies at other wavelengths, and comparable or larger than the evolution rates observed for quasars. Number counts at 15 and 24  $\mu\text{m}$  show a prominent bump peaking at about 0.4 mJy and 0.3 mJy respectively. At the peak of the bump, the counts are more than one order of magnitude above the non-evolution models. At 15  $\mu\text{m}$ , data require a combination of a  $(1+z)^3$  luminosity evolution and  $(1+z)^3$  density evolution for the starburst component at redshift lower than 0.9 to fit the strong evolution. While it has not been possible with *ISOCAM* to probe in detail the evolution of the IR luminosity function, *Spitzer* data at 24  $\mu\text{m}$  give for the first time tight constraints up to redshift 1.2 (Le Floc'h et al. 2005). A strong evolution is noticeable and requires a shift of the characteristic luminosity  $L^*$  by a factor  $(1+z)^{4.0\pm0.5}$ . Le Floc'h et al. (2005) find that the LIRGs and ULIRGs become the dominant population contributing to the comoving IR energy density beyond  $z\sim0.5-0.6$  and represent 70% of the star-forming activity at  $z\sim1$ . Those findings are in good agreement with the predictions from Lagache et al. (2004). This model constrains in a simple way the IR luminosity function evolution with redshift, and fits all the existing source counts consistent with the redshift distribution, the CIB intensity, and, for the first time, the CIB fluctuation observations from the mid-IR to the submillimeter range. In this model, we assume that IR galaxies are mostly powered by star formation and hence we use SEDs typical of star-forming galaxies. Although some of the galaxies will have AGN-dominated SEDs, they are a small enough fraction that they do not affect the results significantly. We therefore construct 'normal' and starburst galaxy template SEDs: a single form of SED is associated with each activity type and luminosity. We assume that the Luminosity Function (LF) is represented by these two activity types and that they evolve independently and we search for the form of evolution that best reproduces the existing data. An example of two cosmological implications of this model is that (1) the PAHs features remain prominent in the redshift band 0.5 to 2.5 and (2) the IR energy output has to be dominated by  $\sim 3 \cdot 10^{11} L_\odot$  to  $\sim 3 \cdot 10^{12} L_\odot$  galaxies from redshift 0.5 to 2.5. The excellent agreement between the model and all the available observational constraints makes this model a likely good representation of the average luminosity function as a function of redshift and a useful tool to discuss observations and models (e.g. figure 3 showing the contribution by redshift to the MIPS 24  $\mu\text{m}$  source counts). Its rather simple assumptions like the single parameter sequence of SEDs for starburst galaxies is certainly not accounting for some of the detailed recent observations (e.g. Lewis et al. 2005) but probably do not affect seriously the redshift evolution of the averaged properties which are what is modeled.

The comoving luminosity density produced by luminous IR galaxies was more than 10 times larger at  $z\sim1$  than in the local Universe. For compari-

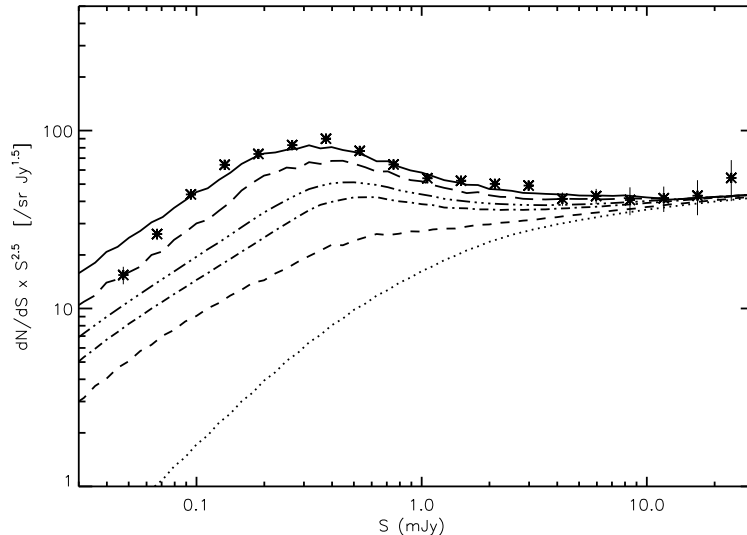


Figure 3. Redshift contribution to the number counts at  $24\ \mu\text{m}$  from the model of Lagache et al. (2004, their figure 7). The dot, dash, dash-dot, dash-3 dot, long-dash correspond to the number counts up to redshifts 0.3, 0.8, 1, 1.3 and 2 respectively. Data are from Papovich et al. (2004).

son, the B-band luminosity density was only 3 times larger at  $z=1$  than today. Such a large number density of LIRGs in the distant Universe could be caused by episodic and violent star formation events, superimposed to relatively small levels of star formation activity (Hammer et al. 2005). These events can be associated to major changes in the galaxy morphologies.

The large fraction of the background resolved at  $850\ \mu\text{m}$  has interesting consequences. It shows very directly that if the sources are at redshift larger than 1 (as confirmed by the redshift surveys), the IR luminosity of the sources dominating the background is larger than  $10^{12}L_{\odot}$ , in agreement with the predictions of Lagache et al. (2004), thus making a population with a very different IR luminosity function than the local or even the  $z=1$  luminosity function. The link between this population at high  $z$  and what has been seen around redshift one (almost by *ISO*) will be done by *Spitzer/MIPS* observations at  $24\ \mu\text{m}$ . *ISO-CAM* galaxies contribute to about 2/3 of the energy peak of the CIB (Elbaz et al. 2002). The remaining fraction is likely to be made of sources in the redshift range 1.5 to 2.5. The presently detected submillimeter galaxies with luminosity  $10^{12}L_{\odot}$  have an almost constant flux between redshift 1.7 and redshift 2.5 at  $24\ \mu\text{m}$  (similar to the constant flux at  $850\ \mu\text{m}$  between redshift 1 and 5). The *MIPS*  $24\ \mu\text{m}$  deep surveys (e.g. Papovich et al. 2004) reach an 80% completeness of  $80\ \mu\text{Jy}$  (and many sources are fainter) and thus can detect all these galaxies when they are starburst-dominated. Considering the efficiency of *MIPS* to cover large areas of the sky with a good sensitivity, it is likely that  $24\ \mu\text{m}$  surveys will become the most effective way to search for luminous starburst galaxies up to  $z=2.5$  and up to 3 for the most luminous ones. In the near future when a

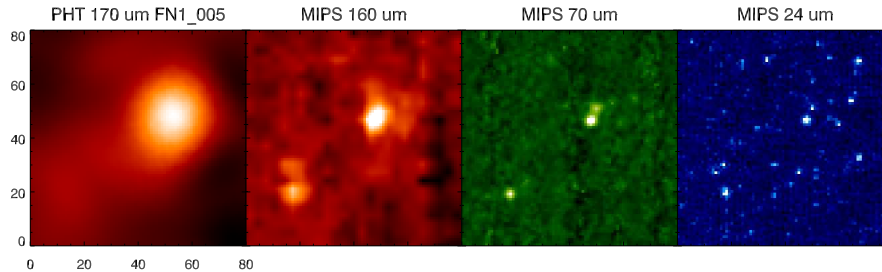


Figure 4. Effects of confusion in the far-IR. Observation of a source in the ELAIS-N1/FIRBACK field, in a 400x400 square arcsecond box. All plates have been resampled to 5 arcseconds per pixel, which oversamples the far IR maps but undersamples the mid-IR map. From left to right: 373 mJy *ISOPHOT* 170  $\mu\text{m}$  source with about 128s of integration (FIRBACK survey, Dole et al., 2001); Labels indicate the 5 arcsecond pixels; *Spitzer MIPS* 160  $\mu\text{m}$  with about 16s of integration (SWIRE survey, Lonsdale et al., 2004); *MIPS* 70  $\mu\text{m}$  with about 80s of integration (SWIRE); *MIPS* 24  $\mu\text{m}$  with about 160s of integration (SWIRE). Notice (1) the *ISO* 170  $\mu\text{m}$  source is marginally resolved with *MIPS* 160, and is unambiguously resolved at 70  $\mu\text{m}$  and 24  $\mu\text{m}$ ; (2) the two fainter *MIPS* 160  $\mu\text{m}$  resolved sources (bottom left) create fluctuations in the *ISO* 170  $\mu\text{m}$  map that produce the confusion noise when the resolution is limited.

proper census of ULIRGs up to  $z \simeq 3$  will be done, the fraction of the CIB at  $\sim 1$  mm not accounted for should give an indication of the contribution from sources at larger redshifts. Deep surveys around 1-2 mm are the only obvious tool to get most of these sources. But the limiting factors of the surveys are not only detector sensitivity or photon noise, there is also confusion.

#### 4. Confusion in the Mid- and Far-Infrared

Even if the term “confusion” might be vague, we can nevertheless define the confusion in general as the degradation of a high spatial frequency signal due to a poor angular resolution (see fig. 4). By degradation, we mean the measurement of a source is affected either by a poorer quality of photometry, or a lower detectability. By high frequency signal we mean small-scale observed structures compared to the beam, usually extragalactic point-sources. Finally, by poor angular resolution, we mean a large beam or a poor point spread function sampling compared to the studied structure, usually a set of point sources.

Predicting or measuring confusion depends on the scientific goal of the measurement (e.g. Helou & Beichman, 1990; Dole et al., 2003; Lagache et al., 2003): performing an unbiased far-IR or submillimeter survey and getting a complete sample has different requirements than following-up in the far-IR an already known near-IR source to get a SED and/or a photometric redshift. In the former case, one has to tightly control the statistical properties of the whole sample; in the latter case, completeness is irrelevant, and an even low photometric accuracy is adequate. We thus favor the use of a qualifier, like “unbiased confusion” for the former case. New techniques are being developed to

use an *a priori* information at shorter wavelength (e.g.  $8\ \mu\text{m}$  with *Spitzer*/IRAC and  $24\ \mu\text{m}$  with *MIPS*, respectively) to infer some statistical properties (like source density or SED) of sources at longer wavelength (e.g.  $24$  or  $160\ \mu\text{m}$ , respectively), and thus to beat the unbiased confusion.

Predicting the unbiased confusion (for instance Condon, 1974; Franceschini et al., 1989; Helou & Beichman, 1990; Rieke et al. 1995; Dole et al., 2003; Lagache et al., 2003; Takeuchi & Ishii, 2004; Negrello et al., 2004) requires the knowledge of at least the number counts distribution of the galaxies. In practice, models (validated at some point by observations) are used. Since the slope of the counts in a  $\text{Log}(N) - \text{Log}(S_\nu)$  diagram is varying with the flux density  $S_\nu$ , the fluctuation level of faint sources below  $S_\nu$  will also vary; this fluctuation level gives an estimate of the unbiased confusion using a photometric criterion (Dole et al., 2003; Lagache et al., 2003). At very faint fluxes, when the background is almost resolved, the photometric criterion will obviously give a very small value for the unbiased confusion level, but the observations will be limited by the confusion due to the high density of faint resolved sources. Thus, another criterion, the source density criterion for unbiased confusion (SDC, Dole et al., 2003, 2004), needs to be computed and compared to the photometric criterion. In the IR and submillimeter range below  $300\ \mu\text{m}$ , the unbiased confusion is in general better predicted by the source density criterion for current and future facilities, since the angular resolution has improved (e.g. from ISO to *Spitzer*). At longer wavelengths, the photometric criterion still dominates.

In Dole et al. (2004b), we derived the confusion limits for MIPS. Using data at  $24$ ,  $70$  and  $160\ \mu\text{m}$ , the source density measured by Papovich et al. (2004) and Dole et al. (2004a) together with the modeling of Lagache et al. (2004) has allowed us to derive the confusion limits for *Spitzer* in the mid to far IR. We tested the model results with a Monte Carlo simulation at  $24\ \mu\text{m}$  and with a fluctuations analysis at all 3 wavelengths (fig. 5). The agreement is uniformly very good. We determined the  $5\text{-}\sigma$  unbiased confusion limits due to extragalactic sources:  $56\ \mu\text{Jy}$ ,  $3.2$  and  $40\ \text{mJy}$  at  $24$ ,  $70$  and  $160\ \mu\text{m}$ , respectively. At  $24$  and  $70\ \mu\text{m}$ , confusion is mostly due to the high density of resolved sources, and at  $160\ \mu\text{m}$ , confusion is mainly due to faint unresolved sources. Studying the FIR fluctuations at this wavelength is thus a tool to constrain the nature of the faint galaxies, beyond the confusion limit.

What can be done with these numbers ? Generally speaking, you should stop integrating down to these levels, unless you know the existence of an object (e.g. from shorter wavelength observations) you want extract photometry from. It might thus be useful to integrate deeper than these limits, but the analysis will require some care. For instance, a sample of detected extragalactic faint sources will likely be highly incomplete; this might be a problem for statistical studies, but this can be ignored (or has to be appropriately quantified) if one wants photometry of known objects.

These numbers were derived both from the data and a model, and they explicitly made the assumption of a Poisson source distribution. Source clustering might in principle bias these estimates. Takeuchi & Ishii (2004) derived analytic formulas taking into account the source clustering, and showed that this effect



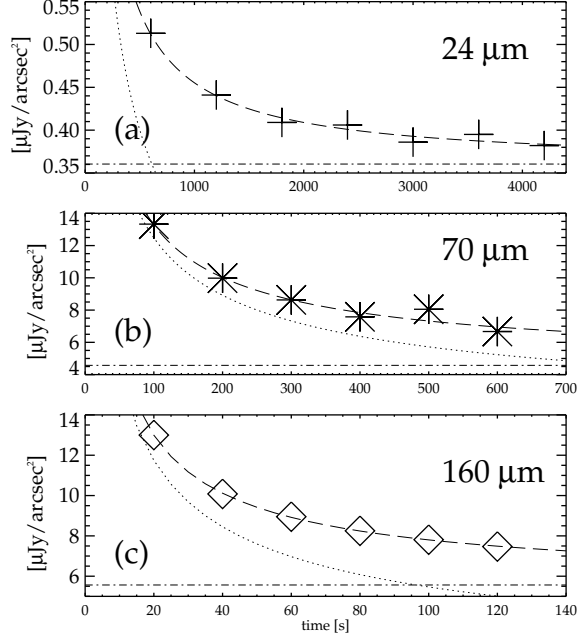


Figure 5. Evolution  $\sigma_{tot}$  (resulting contribution from the confusion noise and instrument noise) as a function of integration time, with a fit (dash) of the form:  $\sigma_{tot}^2 = \sigma_{inst}^2 + \sigma_{conf}^2 = At^{-1} + C^2$ . dot-dash: constant term  $C$ . dot:  $\sqrt{A/t}$  term. Top panel (a):  $24 \mu\text{m}$ . Middle panel (b):  $70 \mu\text{m}$ . Bottom panel (c):  $160 \mu\text{m}$ . Notice the different scales in time (seconds) and  $\sigma_{tot}$  ( $\mu\text{Jy}/\text{arcsec}^2$ ). From Dole et al., 2004b.

is at the  $\sim 10\%$  level.

Confusion is also created in the IR by the presence of Galactic cirrus (Low et al., 1984), even if its complex structure has little power at small scales (Gautier et al., 1992; Herbstmeier et al., 1998; Miville-Deschênes et al., 2003, Kiss et al., 2001 & 2003; Ingalls et al., 2004). Usually, IR cosmological surveys are performed in high Galactic latitude cirrus-free regions, with a column-density as low as possible. For instance, only 2% of the sky have  $N_{HI} \leq 1.0 \times 10^{20} \text{ cm}^{-2}$ . Table 2 gives more details about the fraction of the sky cleaner than certain column-densities. A common problem arises when cosmological fields, chosen in the visible range, happen to fall in high Galactic cirrus contamination fields, avoiding any efficient IR follow-up, like the 22h VIMOS field 2217+0024 with a  $100 \mu\text{m}$  brightness of about  $4 \text{ MJy}/\text{sr}$ .

A number of cryogenically-cooled space telescopes have been proposed for the MIR, the FIR and the submillimeter spectral ranges. Table 2 of Dole et al. (2004b) summarizes the main characteristics of some of these observatories. Herschel (Pilbratt, 2001), JWST (Gardner, 2003), SPICA (Matsumoto, 2003) and SAFIR (Yorke 2002), have at least one photometric channel in common with MIPS. As examples, Dole et al. (2004b) focused on Herschel-PACS at

$N(\text{HI})/cm^{-2}$	Sky Fraction
$\leq 1.0 \times 10^{20}$	2%
$\leq 1.25 \times 10^{20}$	5%
$\leq 1.6 \times 10^{20}$	10%
$\leq 2.0 \times 10^{20}$	17%
$\leq 2.2 \times 10^{20}$	20%
$\leq 3.0 \times 10^{20}$	30%
$\leq 3.8 \times 10^{20}$	40%
$\leq 5.0 \times 10^{20}$	52%

Table 2. Fraction of the sky with HI column-densities lower than certain values. These numbers are derived from the HI Burton & Hartman (1994) Leiden/Dwingeloo survey, assuming an all sky coverage.

75 and 170  $\mu\text{m}$ , on JWST-MIRI at 24  $\mu\text{m}$ , and on SPICA and SAFIR at 24, 70 and 160  $\mu\text{m}$ , assuming in each case that the MIPS filters will be used. In Table 3 of Dole et al. (2004b), we use the confusion level given by the SDC, and compute the fraction of the CIB potentially resolved into sources. In the MIR, a significant step will be made with the 4m-class space telescope: as an example, SPICA would potentially resolve 98% of the CIB at 24  $\mu\text{m}$ . All ( $> 99\%$ ) of the CIB would be resolved with JWST or SAFIR (although doing so with JWST would require extremely long integrations). In the FIR, Herschel would resolve a significant fraction of the CIB at 70 and 160  $\mu\text{m}$  (resp. 93 and 58%, again with extremely long integrations). SAFIR will ultimately nearly resolve all of it ( $> 94\%$ ).

Predictions of the unbiased confusion, for various telescope diameters and wavelengths, will be soon available on our website<sup>1</sup>.

## 5. Beating the Unbiased Confusion

Observing in the FIR and submm spectral ranges is relevant to characterize the galaxies responsible of the CIB at redshifts  $z \geq 1.3$  (Table 1) but the unbiased confusion usually avoids to directly probe these galaxies. What can be done ? As already mentioned, one method consists in extrapolating the FIR and submm properties of the galaxies from the MIR (or from the radio) spectral properties, based on controlled samples having FIR and submm data. These controlled samples are usually small (e.g. Appleton et al., 2004). This has the advantage of allowing to apply this extrapolation to large samples like the new IRAC or MIPS catalogs from GTO or legacy surveys, but the disadvantage of being dependent on the extrapolation based on a small sample, and of not allowing any object by object study. More observations are thus required in the FIR and submm to extend these controlled samples; more *Spitzer* GO programs should address this need in the near future.

---

<sup>1</sup><http://lully.as.arizona.edu/Model>

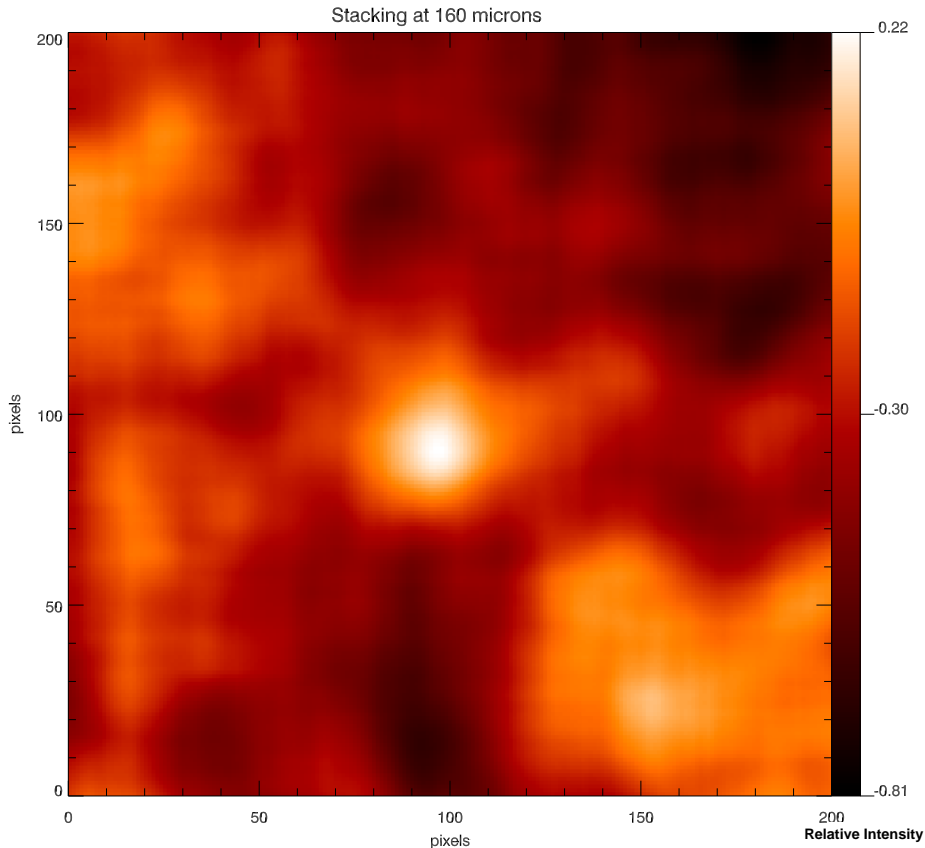


Figure 6. Example of a stacking analysis at  $160\ \mu\text{m}$ .  $24\ \mu\text{m}$  sources in the CDFS are selected to have flux densities  $80 \leq S_{24} \leq 83\ \mu\text{Jy}$  (330 sources). Images at  $160\ \mu\text{m}$  are stacked at the positions of the  $24\ \mu\text{m}$  sources. There is a clear detection in the resulting stacked  $160\ \mu\text{m}$  image in the center, with the expected FWHM. Pixel scale here is  $1.25\ \text{arcseconds/pixel}$ .

Another method consists in characterizing already known submm (or FIR) sources. Egami et al. (2004) studied VLA and SCUBA sources in the NIR and MIR, and Ivison et al. (2004) did the same of MAMBO  $1.2\text{mm}$  sources and both showed that IRAC and MIPS quickly detect high redshift ( $0.5 \leq z \leq 3.5$ ) massive galaxies, dominated by star formation. Although being successful, this method rely also on small samples.

Finally, a powerful method consists in making biased observations: using shorter wavelength data (like IRAC  $8.0\ \mu\text{m}$  or MIPS  $24\ \mu\text{m}$ ) or high angular resolution data (e.g. VLA  $1.4\ \text{GHz}$ ) to select a physically homogeneous sample, one can extract photometry in the FIR or submm. If the targets fluxes are below the MIPS FIR or SCUBA submm detection limits, one can make use of a stacking analysis to increase the S/N of FIR or submm data. Frayer et al. (2004) used this technique to extract color properties of SCUBA galaxies at  $70\ \mu\text{m}$ . Also, Sergeant et al. (2004) stacked  $450$  and  $850\ \mu\text{m}$  images at the positions of IRAC  $5.8$  &  $8\ \mu\text{m}$  sources, and detected a positive deviation,

allowing them to give a constrain on the contribution of IRAC sources to the submm CIB.

We present here an example of such stacking analysis at  $160\ \mu\text{m}$  for illustration. We first selected a sample of  $24\ \mu\text{m}$  galaxies with flux densities  $80 \leq S_{24} \leq 83\ \mu\text{Jy}$  in the CDFS, and found 330 sources (Papovich et al., 2004). We then stacked the corresponding  $160\ \mu\text{m}$  data. Figure 6 shows the result of a clear detection. This illustrates the power of stacking analysis to probe fainter galaxy population using an *a priori* information from shorter wavelengths.

Not only we can probe individual galaxies deeper into the confusion in the MIR using an *a priori* information at shorter wavelength (e.g. NIR), but we can also probe galaxies statistically in the FIR. In this case, obviously a careful sample selection is required to interpret the resulting photometry.

## 6. Conclusion

The Cosmic Infrared Background, peaking in the FIR, is made of contributions by galaxies located at different redshifts. The FIR CIB has most contribution from  $0.5 \leq z \leq 1.5$  LIRGs, and the submm has most contributions from  $z \geq 2$  ULIRGs. The FIR properties of these IR bright galaxies are not known in detail, mainly because of the unbiased confusion in this spectral range. New *Spitzer* results are starting to refine our knowledge of these galaxies. Beating the unbiased confusion is one of the challenges of the analysis of today's cosmological surveys, and early results show that many methods are promising and successful.

Furthermore, the efficiency of MIPS  $24\ \mu\text{m}$  to cover large sky areas to a great depth is a unique tool to search high redshift ULIRGs responsible of the submm CIB. There might be another *Spitzer* legacy consisting to cover wider areas to pinpoint this population, which might be characterized using also submm data from Herschel (and Planck), either on an individual basis or statistically.

**Acknowledgments.** We wish to thank the organizers. Special thanks to the MIPS GTO team for a fruitful and enjoyable collaboration. Thanks to the FLS, SWIRE and GOODS teams, as well as IRAC, IRS and SSC people, for the great work providing the community with outstanding *Spitzer* data.

## References

- Appleton P. N., Fadda D. T., Marleau F. R., et al., 2004, *ApJS*, 154, 147
- Armand C., Milliard B., Deharveng J. M., 1994, *A&A*, 284, 12
- Bernstein R. A., Freedman W. L., Madore B. F., 2002, *ApJ* 571, 56
- Burton W. B. & Hartman D., 1994, *ApSS*, 217, 189
- Chanial P., 2003, PhD Thesis
- Chapman S. C., Blain A. W., Ivison R. J., Smail I., 2003, contributed talk at "Star formation through time", Granada Spain, Oct.2002
- Dole H., Gispert R., Lagache G., et al., 2001, *A&A*, 372, 364
- Dole H., Lagache G., Puget J-L., 2003, *ApJ*, 585, 617
- Dole H., Le Floc'h E., Pérez-González P. G. et al., 2004, *ApJS*, 154, 87
- Dole H., Rieke G. H., Lagache G., et al. , 2004, *ApJS*, 154, 93
- Egami, E., Dole H., Huang J. S., et al., 2004, *ApJS*, 154, 130
- Elbaz D., Le Floc'h E., Dole H., Marcillac D., 1005, *A&A*, in press
- Elbaz D., Cesarsky C. J., Chanial P. et al., 2002, *A&A* 384, 848

- Elbaz D., Cesarsky C., Fadda D., et al., 1999, *AA*, 351, L37
- Franceschini A., Toffolatti, L., Danese L., & De Zotti G., 1989, *ApJ*, 344, 35
- Frazer D. T., Chapman S. C., Yan L., et al., 2004, *ApJS*, 154, 137
- Gautier N. T., Boulanger F., Perault M., Puget J.-L. *ApJ*, 103, 1313
- Gispert R., Lagache G., Puget J.-L., 2000, *A&A* 360, 1
- Gardner J. P., 2003, IAU, Joint Discussion 8, 10
- Gorjian V., Wright E. L., Chary R.R., 2000, *ApJ* 536, 550
- Hammer F., Flores H., Elbaz D., et al., 2005, *A&A*, 430, 115
- Hauser M., and Dwek E., 2001, *Ann. Rev. Astron. Astrophys.* 37, 249
- Hauser M. G., Arendt R. G., Kelsall T., et al., 1998, *ApJ* 508, 25
- Helou G. & Beichman C. A., 1990, ESA SP-314 “From Ground-Based to Space-Borne Sub-mm Astronomy”, ESA, 117
- Herbstmeier U., Abraham P., Lemke D., et al., 1998, *A&A*, 332, 739
- Ingalls J. G., Miville-Deschênes M.-A., Reach W. T., et al., 2004, *ApJS* 154, 281
- Ivison R. J., Greve T. R., Serjeant S., et al., 2004, *ApJS* 154, 124
- Kiss C., Abraham P., Klaas U., et al., 2001, *A&A*, 379, 1161
- Kiss C., Abraham P., Klaas U., et al., 2003, *A&A*, 399, 177
- Lagache G., Puget J.-L., Dole H., 2005, *ARAA*, in press
- Lagache G., Dole H., Puget J.-L. et al., 2004, *ApJS* 154, 112
- Lagache G., Dole H., Puget J.-L. et al., 2003, *MNRAS*, 338, 555
- Lagache G., Haffner L. M., Reynolds R. J., Tufte S.L., 2000, *A&A* 354, 247
- Le Floc’h E., Papovich C., Dole H., et al. 2005, *ApJ*, to be submitted
- Lewis G. F., Chapman S. C., Helou G., 2005, *ApJ*, in press
- Liang Y. C., Hammer F., Flores H., et al. 2004, *A&A* 423, 876
- Lonsdale, C. J., Polletta M., Surace J., et al., 2004, *ApJS*, 154, 54
- Low F. J., Young E., Beintema D. A., et al., 1984, *ApJ*, 278, L19
- Matsumoto T., 2003, SPIE, 4850, 1091
- Miville-Deschênes M.-A., Lagache, G., Puget J.-L., 2002, *A&A* 393, 749
- Miville-Deschênes M.-A., Joncas G., Falgarone E., Boulanger F., 2003, *A&A*, 411, 109
- Negrello M., Magliocchetti M., Moscardini L., et al., 2004, *MNRAS*, 352, 493
- Papovich C., Dole H., Egami E., et al, 2004, *ApJS* 154, 70
- Pérez-González P. G. et al., *ApJ*, submitted
- Pilbratt G. L., 2001, ESA-SP 460, 13
- Puget J.L., Abergel A., Bernard J.P., et al., 1996, *A&A* 308, L5
- Renault C., Barrau A., Lagache G., Puget J.-L., 2001, *A&A* 371, 771
- Rieke G. H., Young E. T., & Gautier T. N., 1995, *Space Sci. Rev.*, 74, 17
- Serjeant, S., Mortier A. M. J., Ivison R. J., et al., 2004, *ApJS*, 154, 118
- Smail I., Ivison R. J., Blain A. W., Kneib J.-P., 2002, *MNRAS* 331, 495
- Soifer B. T., Neugebauer G., 1991, *AJ* 101, 354
- Takeuchi T. T & Ishii, T. T., 2004, *ApJ*, 604, 40
- Wright E. L., 2001, *ApJ* 553, 538
- Yorke H. W., Bock J. J., Dragovan M. W., et al., 2002, AAS, 2011, 5104